Calibrated Polarisation Tilt Angle Recovery for Wireless Communications

Vincent Fusco, *Fellow, IEEE,* and Dmitry Zelenchuk, *Senior Member, IEEE*

***Abstract*— In this paper, we show how the polarisation state of a linearly polarised antenna can be recovered through the use of a three-term error correction model. The approach adopted is shown to be robust in situations where some multipath exists and where the sampling channels are imperfect with regard to both their amplitude and phase tracking. In particular, it has been shown that error of the measured polarisation tilt angle can be improved from 33% to 3% and below by applying the proposed calibration method. It is described how one can use a rotating dipole antenna as both the calibration standard and as the polarisation encoder, thus simplifying the physical arrangement of the transmitter. Experimental results are provided in order to show the utility of the approach, which could have a variety of applications including bandwidth conservative polarisation sub-modulation in advanced wireless communications systems.**

***Index Terms*—polarisation estimation, calibration.**

I. Introduction

POLARISATION state encoding offers a bandwidth efficient means for carrying information. It has been proposed in [1] for transmission of data over fibre optic cables. In [1] it was shown that multi-level polarisation encoded signals could be effective in coherent optical modulation systems. With such systems the encoding and decoding strategies involved are rather complex and generally unsuitable for wireless communications.

The use of polarisation states to encode information yields additional degrees of freedom for spectrum-hungry wireless systems. In [2] a thorough analysis of using polarisation state encoding for multiple access line-of-sight wireless systems was performed and potential encoding and decoding strategies proposed. As with the techniques developed for the optical schemes the decoding strategies developed in [2] are rather complex and rely on advanced signal processing methods as well as the fact that the polarisation states are known to the system. In [3] it was shown how circular polarisation could be used to encode m-level digital states on an LOS wireless link and how decoding could be achieved using channel phase compensation. In order for these techniques to be useful for wireless communications in a realistic environment, a robust and simple method for determination of the polarisation states without a prior knowledge of the channel properties is necessary.

For such purposes the radar community has exploited, e.g. [4], the techniques used for the calibration of vector network analysers (VNAs). Here, radar cross section measurements are conducted using radar absorber, and metal objects as calibration loads. This technique allows removing systematic errors due to the frequency response of the hardware, source impedance matching and residual echo from the chamber background. The method proceeds by using the one-port error correction strategy described in [5] for the calibration of a VNA. In [6] the analogy between one port VNA calibration and polarisation ratio was developed. The method proposed can be useful for recovering polarisation states. In this paper, we examine experimentally for the first time the proposal made in [6] in different scenarios and study effects of various sources of error on the recovered polarisation states.

Section II of this paper describes the analogy between the one-port error model and the measurement of polarisation ratio, as well as the use of a rotating dipole both as a calibration set and as a data encoder. Section III describes the simulated and measured results obtained to validate the analysis in Section II. In Section IV the effects that systematic hardware errors and additive white Gaussian noise have on the measurement are described.

II. Analogy between VNA one port error model and polarisation ratio

In [6] an analogy between the incident and reflected waves present at the measurement port of a network analyser bi-directional coupler and the orthogonally polarised electric fields from a transmitting antenna was developed. Once established this allows direct application of one-port network analyser error correction method for the purposes of recovering the polarisation ratio of the two orthogonal electric fields radiated by the antenna under test. This is done by means of a remote measurement made using a sampling antenna pair and single switched receiver or dual receiver system. The sampling antenna pair and the receiver configuration can be imperfect in regards to polarisation purity and channel tracking respectively.

The complex polarisation ratio is defined as $\rho = E_q/E_p$. This is the ratio between the two orthogonal components of an electromagnetic wave coming from an antenna under test. These components will carry information about the tilt angle of a linearly polarised signal. We assume that the polarisation tilt

This work was funded by the UK Engineering and Physical Research Council under grant "Informed RF for 5G and Beyond", EP/N020391/1. V. Fusco, and D. Zelenchuk, are with ECIT, Queen's University of Belfast, United Kingdom. (e-mail: v.fusco@ee.qub.ac.uk, d.zelenchuk@qub.ac.uk).

angle is used to wirelessly convey m-level baseband digital data to a remote location. At the remote location the antenna and receiver are employed to recover the encoded transmitted signal.

The objective of this study is to recover the transmitted data at high fidelity despite propagation path effects and hardware imperfections at the receiver with minimum mathematical post-processing of the recovered signals.

Fig. 1 (a) shows a coupler error network superimposed between the load to be measured and the measurement port. Here C_{1i} and C_{2r} are the direct coupling paths whereas c_{1i} and c_{2r} represent the cross-coupling paths. Using this representation one can write (1)

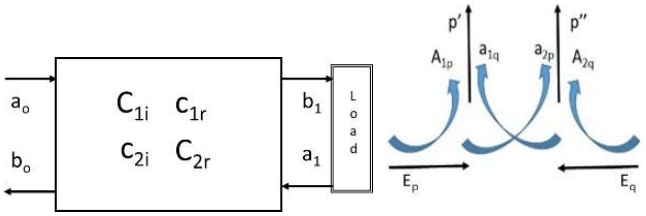

(a) (b)

Fig. 1 Bi-directional coupler and polarisation ratio analogy. (a) - bi-directional coupler; (b) - polarisation analogy

$$\begin{bmatrix} b_0 \\ b_1 \end{bmatrix} = \begin{bmatrix} \frac{c_{2i}}{C_{1i}} & -\frac{c_{2i}c_{1r}}{C_{1i}} + c_{2r} \\ \frac{1}{C_{1i}} & -\frac{c_{1r}}{C_{1i}} \end{bmatrix} \begin{bmatrix} a_0 \\ a_1 \end{bmatrix} \quad (1)$$

and we know from [5] that

$$\begin{bmatrix} b_0 \\ b_1 \end{bmatrix} = \begin{bmatrix} e_{00} & e_{01} \\ e_{10} & e_{11} \end{bmatrix} \begin{bmatrix} a_0 \\ a_1 \end{bmatrix} \quad (2)$$

and

$$\Delta e = e_{00}e_{11} - e_{10}e_{01} = \frac{c_{2r}}{C_{1i}} \quad (3)$$

Hence, after [5], the true reflection coefficient Γ can be extracted from the measured reflection coefficient Γ_m as

$$\Gamma = \frac{\Gamma_m - e_{00}}{\Gamma_m e_{11} - \Delta_e} \quad (4)$$

Provided three loads $\Gamma_{m_{i=1,2,3}}$ are known, then three simultaneous equations result from which the error coefficients e_{00} , e_{11} and Δ_e can be obtained.

Consider now an antenna radiating into the far field with electric field components E_p , E_q, Fig.1b. If the signals measured in two channels (or a time multiplexed single channel) by imperfect sampling antennas connected to imperfect hardware are denoted as $\overrightarrow{A_1}$ and $\overrightarrow{A_2}$, respectively, then after [6] one can write

$$\begin{aligned} \overrightarrow{A_1} &= \overrightarrow{u_p}\, A_{1p} + \overrightarrow{u_q} a_{1q} \\ \overrightarrow{A_2} &= \overrightarrow{u_p}\, a_{2p} + \overrightarrow{u_q} A_{2q} \end{aligned} \quad (5)$$

where A_{1p} and A_{2q} are the measured co-polar components whereas a_{1q} and a_{2p} are the measured cross-polar components; $\overrightarrow{u_p}$ and $\overrightarrow{u_p}$ are the orthogonal polarisation vectors. The A_{1p}, A_{2q} and a_{1q}, a_{2p} coefficients are respectively equivalent to the error network coefficients C_{1p}, C_{2q} and c_{1q}, c_{2p}.

Thus by analogy with (1) and (4)

$$\begin{aligned} e_{00} &= \frac{a_{2P}}{A_{1p}} \\ e_{11} &= \frac{-a_{1q}}{A_{1p}} \\ \Delta e &= -\frac{A_{2q}}{A_{1p}} = e_{00}e_{11} - e_{10}e_{01} \end{aligned} \quad (6)$$

and the error corrected polarisation ratio ρ is

$$\rho = \frac{\rho_m - e_{00}}{\rho_m \rho_{11} - \Delta_e} \quad (7)$$

Following [5], three error factors are necessary to accomplish the polarisation calibration. These three factors are obtained from system of three equations retrieved from calibration standard measurements

$$e_{00} + \rho_i\, \rho_{m_i}\, e_{11} - \rho_i\, \Delta e = \rho_{m_i} \quad (8)$$

where ρ_{m_i} is measured value of the calibration standard with known ideal value ρ_i. From these three coefficients any new measured ρ_m can be calibrated to the true value ρ by solving (8). The tilt angle is then recovered as

$$\beta = \operatorname{atan} \Re(\rho) \quad (9)$$

With the above approach, one can use a single rotating linearly polarised dipole or slot antenna as both the calibration load set and the data encoder. The dipole or slot can be mechanically rotated or electronically rotated, e.g. [7]. Table 1 shows how a linear dipole can be positioned at various orientation angles so that its radiation in the far field constitutes the three polarisation states: + 1, 0, - 1 that are equivalent to the three-term error correction loads open circuit, short circuit and load. From these three polarisation calibration coefficients ρ_m we can establish the polarisation ratio for any arbitrarily rotated dipole.

TABLE I
POLARISATION STATES

Dipole Orientation	Dipole Polarisation	Calibration load Value	Error Coefficient
$1\angle 0°$	LP_y	$\rho_1 = 0$	$e_{00} = 0$
$1\angle +45°$	LP_{+45}	$\rho_2 = +1$	$e_{11} = 0$
$1\angle -45°$	LP_{-45}	$\rho_3 = -1$	$\Delta e = +1$

* E_p used as reference channel $E_p \geq E_q$: $\rho = \frac{E_q}{E_p}$

III. Simulated and Measured Results

A. Simulation: ideal sampling probes

As a first test for the approach, we perform full-wave simulations of a straight half-wave dipole. The half-wave transmit dipole is rotated by angle θ with respect to axis x and two orthogonal sampling probes are placed in its far field. The dipole length l = 46 mm, feed gap g = 0.5 mm. The resonant frequency of the dipole is 3 GHz, and all simulations were conducted using CST Microwave Studio.

This dipole functions as both the data-carrying transmitter and as the calibration standards for the system. The ideal orthogonal E-field sampling probes are used to represent a perfect receiver. After the calibration procedure described in Section II was applied, the calibration error between the ideal and simulated calibration standards was plotted in Fig. 2a. Here it can be seen that for this nearly perfect scenario the residual error post calibration is very low.

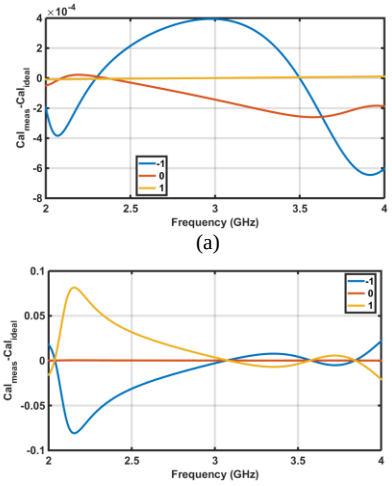

(a)

(b)

Fig. 2 Calibration error: (a) - ideal E-field probe receive sampler, (b) - dipole receive sampler

B. Simulation: sampling with a dipole

In the next simulation, the same linearly polarised dipole was used as before and this time, the received field is sampled with an identical linearly polarised dipole antenna as was used at the transmitter. The receive dipole is aligned with the x-axis to sample the x directed E-field component and is then rotated by 90° to sample y directed E-field component, thereby eliminating cross polar contamination of the sampled E-field components. Fig. 2b shows that the error in the calibration coefficients obtained is small.

C. Measurement: anechoic environment

In the measurement, two dipoles were used. The transmit dipole is attached to a rotary joint and can take any arbitrary orientation including the prescribed calibration orientations, +45°, 0°, -45°. Initially, all tests were conducted in an anechoic chamber. The manufactured dipoles used for transmitting and receiving in the experiment had nearly identical far-field radiation characteristics and return loss below -15 dB at 3 GHz. The experiments were performed for ±90° rotation span with 5° step. For brevity, a sample result for the tilt angle of -30° is presented in Fig. 3 when the arrangement is operated in a 10 m anechoic chamber. It can be seen that post calibration the recovered tilt angle error is reduced to below ± 0.5°, while in the non-calibrated case the error can rise to as much as 10° away from the resonant frequency of the transmit antenna.

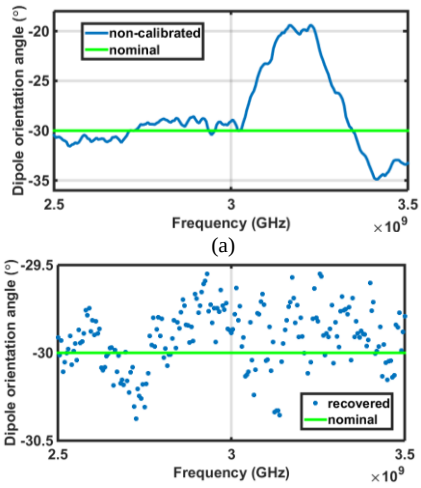

(a)

(b)

Fig. 3 Example orientation extraction for -30° rotated dipole in a fully anechoic environment: (a) – no calibration, (b) – post calibration.

D. Measurement: partially anechoic environment

Next, we look at the results, Fig. 4, for the scenario where some multipath can exist. Here we make our measurements in a partially anechoic environment, namely the anechoic chamber above with a metallic floor. The antennas are positioned at 60 cm height above the uncovered metallic floor. It can be seen that post calibration the recovered tilt angle error is reduced to below ±1°, while in the non-calibrated case the error can rise to as much as 10° away from the resonant frequency of the transmit antenna. Results for other orientation angles for both anechoic and non-anechoic situations are similar to those presented here in Fig. 3, 4.

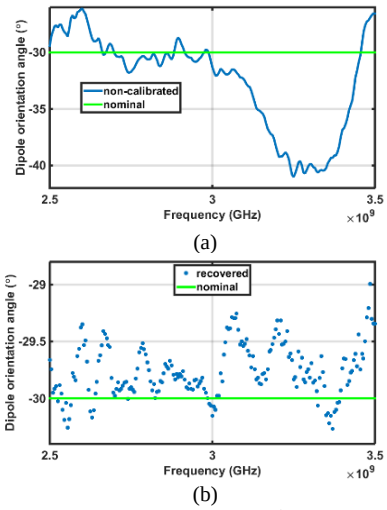

(a)

(b)

Fig. 4 Example sample orientation extraction for -30° dipole in the partially anechoic environment: (a) – no calibration, (b) – post calibration.

IV. Effect of Systematic Hardware Errors and AWGN

We next investigate the robustness of the method to hardware

defects such as amplitude and phase imbalances on the receive chain including any additional error introduced by cross-polar contamination in the sampling and calibration standard antennas. In order to simulate this, we operate on all previously measured data using $\rho_{in} = e\ \rho_m$ where e is a complex weight, $|e| = 0.3 \ldots 1,\ \angle e = 0..\frac{\pi}{4}$. It was found that the values of the data extracted were entirely unaffected due to the capacity of the error correction scheme to mitigate systematic error.

Furthermore, we investigated how the recovered orientation angle is affected by additive Gaussian noise, AGWN, added by the channel and superimposed on both components of the measured electric field according to

$$E_{xn} = E_x + n_x, \quad E_{yn} = E_y + n_y \tag{10}$$

where n_x and n_y is additive noise. We assume that the noise for both components are two different stationary processes each with Gaussian distribution and the same mean $\mu = 0$ and variance $\sigma(SNR)$, which is added to the measured data. The power of the signal is calculated as $P_s = \frac{1}{2}\left(|E_x|^2 + |E_y|^2\right)$ and signal-to-noise ratio SNR computed. The recovered orientation angle is shown in Fig. 5.

One can see that the addition of AWGN cannot be removed by the calibration procedure due to its random nature. We note that for SNR = 10 dB we can recover tilt angle out to ±50º, and at SNR = 30 dB out to ±85º with the error of ±3º By increasing SNR to 50 dB the error is reduced to ±1º.

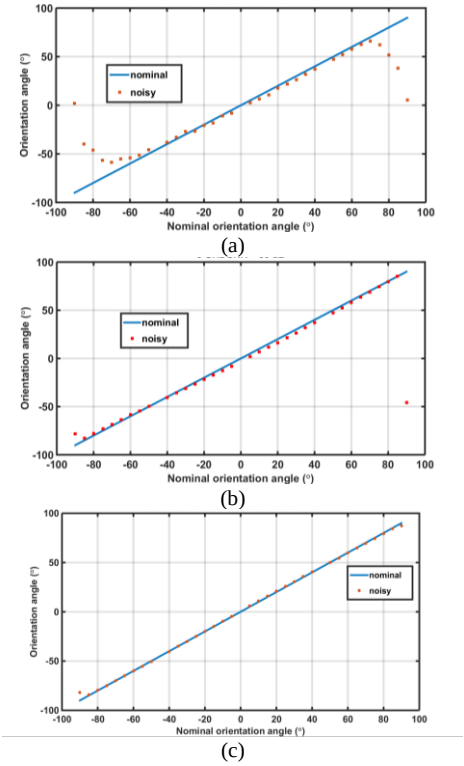

(a) (b) (c)

Fig. 5 Effect of AGWN, on recovered orientation angle. SNR equals to (a) 10 dB, (b) 30 dB, (c) 50 dB.

Thus, the presence of AWGN will limit the range of polarisation states that can ultimately be encoded by this method. This result is expected, since the three-port error model cannot correct for non-systematic errors, as can be seen by examination of (6) with AGWN μ added, (11).

$$e_{00} = \frac{a_{2P} + \mu'}{A_{1P} + \mu'}, \quad e_{11} = \frac{-a_{1q} + \mu''}{A_p + \mu'}, \quad \Delta e = -\frac{A_{2q} + \mu''}{A_{1p+}\mu'} \tag{11}$$

Here we assume that the noise in the channel consists of two AGWN processes μ', μ'' with zero mean and the same variance. Consequently, both e_{11} and Δe coefficients are separately affected by the AGWN processes that do not cancel out.

ACKNOWLEDGMENTS

The authors are grateful to Mr Kieran Rainey for his help with the measurements.

V. CONCLUSION

In this paper, we have described the application of a simple method for the purpose of extraction of polarisation tilt angle for a signal in free-space, multipath and noisy environments. In particular, it has been shown that error of the measured polarisation tilt angle can be improved from 33% to 3% and below by applying the proposed calibration method. The noise level is shown to be of particular concern. It has been demonstrated that by improving SNR from 10 to 30 dB one can increase the span of recovered angles from ±50º to ±85º with the error of ±3º, and reduce the error to ±1º by improving SNR to 50 dB. The experimental results obtained are of interest for bandwidth conservative wireless systems with polarisation encoded signals as the method does not require complex mathematical processing, thus hardware complexity reducing of transmitter and receiver.

REFERENCES

[1] S. Benedetto and P. Poggiolini, "Theory of polarization shift keying modulation," *IEEE Trans. Commun.*, vol. 40, no. 4, pp. 708–721, Apr. 1992.

[2] B. Cao, Q.-Y. Zhang, and L. Jin, "Polarization division multiple access with polarization modulation for LOS wireless communications," *EURASIP J. Wirel. Commun. Netw.*, vol. 77, 2011.

[3] Z. Ul Abidin, P. Xiao, M. Amin, and V. Fusco, "Circular Polarization Modulation for Digital Communication Systems," in *8th International Symposium on Communication Systems, Networks & Digital Signal Processing (CSNDSP)*, 2012, pp. 1–6.

[4] B. K. Chung, H. T. Chuah, and J. W. Bredow, "A microwave anechoic chamber for radar-cross section measurement," *IEEE Antennas Propag. Mag.*, vol. 39, no. 3, pp. 21–26, Jun. 1997.

[5] D. Rytting, "An Analysis of Vector Measurement Accuracy Enhancement Techniques." [Online]. Available: www.hparchive.com/seminar_notes/a-217.pdf. [Accessed: 08-Jun-2016].

[6] J. Budin, "An Automatic Error Correction Method for Measurement of Antenna Polarization," in *13th European Microwave Conference, 1983*, 2006, pp. 845–850.

[7] V. Fusco, O. Malyuskin, and G. Wolosinski, "2-bit polarisation agile antenna with high port decoupling," *Electron. Lett.*, vol. 52, no. 4, pp. 255–256, Feb. 2016.